

Intermittency and Correlations in Hadronic Z^0 Decays

The OPAL Collaboration

Abstract

A multidimensional study of local multiplicity fluctuations and multiparticle correlations of hadrons produced in Z^0 decays is performed. The study is based on the data sample of more than 4×10^6 events recorded with the OPAL detector at LEP. The fluctuations and correlations are analysed in terms of the normalized scaled factorial moments and cumulants up to the fifth order. The moments are observed to have intermittency-like behaviour, which is found to be more pronounced with increasing dimension. The large data sample allows for the first time a study of the factorial cumulants in e^+e^- annihilation. The analysis of the cumulants shows the existence of genuine multiparticle correlations with a strong intermittency rise up to higher orders. These correlations are found to be stronger in higher dimensions. The decomposition of the factorial moments into lower-order correlations shows that the dynamical fluctuations have important contributions from genuine many-particle correlations. The Monte Carlo models JETSET 7.4 and HERWIG 5.9 are found to reproduce the trend of the measured moments and cumulants but they underestimate the magnitudes. The results are found to be consistent with QCD jet formation dynamics, although additional contributions from other mechanisms in the hadronization process cannot be excluded.

(Submitted to European Physical Journal C)

G. Abbiendi², K. Ackerstaff⁸, G. Alexander²³, J. Allison¹⁶, N. Altekamp⁵, K.J. Anderson⁹,
 S. Anderson¹², S. Arce¹⁷, S. Asai²⁴, S.F. Ashby¹, D. Axen²⁹, G. Azuelos^{18,a}, A.H. Ball¹⁷,
 E. Barberio⁸, R.J. Barlow¹⁶, J.R. Batley⁵, S. Baumann³, J. Bechtluft¹⁴, T. Behnke²⁷,
 K.W. Bell²⁰, G. Bella²³, A. Bellerive⁹, S. Bentvelsen⁸, S. Bethke¹⁴, S. Betts¹⁵, O. Biebel¹⁴,
 A. Biguzzi⁵, V. Blobel²⁷, I.J. Bloodworth¹, P. Bock¹¹, J. Böhme¹⁴, D. Bonacorsi²,
 M. Boutemur³⁴, S. Braibant⁸, P. Bright-Thomas¹, L. Brigliadori², R.M. Brown²⁰,
 H.J. Burckhart⁸, P. Capiluppi², R.K. Carnegie⁶, A.A. Carter¹³, J.R. Carter⁵, C.Y. Chang¹⁷,
 D.G. Charlton^{1,b}, D. Chrisman⁴, C. Ciocca², P.E.L. Clarke¹⁵, E. Clay¹⁵, I. Cohen²³,
 J.E. Conboy¹⁵, O.C. Cooke⁸, C. Couyoumtzelis¹³, R.L. Coxe⁹, M. Cuffiani², S. Dado²²,
 G.M. Dallavalle², R. Davis³⁰, S. De Jong¹², A. de Roeck⁸, P. Dervan¹⁵, K. Desch⁸, B. Dienes^{33,d},
 M.S. Dixit⁷, J. Dubbert³⁴, E. Duchovni²⁶, G. Duckeck³⁴, I.P. Duerdoth¹⁶, P.G. Estabrooks⁶,
 E. Etzion²³, F. Fabbri², A. Fanfani², M. Fanti², A.A. Faust³⁰, F. Fiedler²⁷, M. Fierro², I. Fleck⁸,
 R. Folman²⁶, A. Frey⁸, A. Fürstjes⁸, D.I. Futyan¹⁶, P. Gagnon⁷, J.W. Gary⁴, J. Gascon¹⁸,
 S.M. Gascon-Shotkin¹⁷, G. Gaycken²⁷, C. Geich-Gimbel³, G. Giacomelli², P. Giacomelli²,
 V. Gibson⁵, W.R. Gibson¹³, D.M. Gingrich^{30,a}, D. Glenzinski⁹, J. Goldberg²², W. Gorn⁴,
 C. Grandi², K. Graham²⁸, E. Gross²⁶, J. Grunhaus²³, M. Gruwé²⁷, G.G. Hanson¹²,
 M. Hansroul⁸, M. Hapke¹³, K. Harder²⁷, A. Harel²², C.K. Hargrove⁷, M. Hauschild⁸,
 C.M. Hawkes¹, R. Hawkings²⁷, R.J. Hemingway⁶, M. Herndon¹⁷, G. Herten¹⁰, R.D. Heuer²⁷,
 M.D. Hildreth⁸, J.C. Hill⁵, P.R. Hobson²⁵, M. Hoch¹⁸, A. Hocker⁹, K. Hoffman⁸, R.J. Homer¹,
 A.K. Honma^{28,a}, D. Horváth^{32,c}, K.R. Hossain³⁰, R. Howard²⁹, P. Hütemeyer²⁷,
 P. Igo-Kemenes¹¹, D.C. Imrie²⁵, K. Ishii²⁴, F.R. Jacob²⁰, A. Jawahery¹⁷, H. Jeremie¹⁸,
 M. Jimack¹, C.R. Jones⁵, P. Jovanovic¹, T.R. Junk⁶, J. Kanzaki²⁴, D. Karlen⁶,
 V. Kartvelishvili¹⁶, K. Kawagoe²⁴, T. Kawamoto²⁴, P.I. Kayal³⁰, R.K. Keeler²⁸, R.G. Kellogg¹⁷,
 B.W. Kennedy²⁰, D.H. Kim¹⁹, A. Klier²⁶, T. Kobayashi²⁴, M. Kobel^{3,e}, T.P. Kokott³,
 M. Kolrep¹⁰, S. Komamiya²⁴, R.V. Kowalewski²⁸, T. Kress⁴, P. Krieger⁶, J. von Krogh¹¹,
 T. Kuhl³, P. Kyberd¹³, G.D. Lafferty¹⁶, H. Landsman²², D. Lanske¹⁴, J. Lauber¹⁵,
 S.R. Lautenschlager³¹, I. Lawson²⁸, J.G. Layter⁴, D. Lazic²², A.M. Lee³¹, D. Lellouch²⁶,
 J. Letts¹², L. Levinson²⁶, R. Liebisch¹¹, B. List⁸, C. Littlewood⁵, A.W. Lloyd¹, S.L. Lloyd¹³,
 F.K. Loebinger¹⁶, G.D. Long²⁸, M.J. Losty⁷, J. Lu²⁹, J. Ludwig¹⁰, D. Liu¹², A. Macchiolo²,
 A. Macpherson³⁰, W. Mader³, M. Mannelli⁸, S. Marcellini², C. Markopoulos¹³, A.J. Martin¹³,
 J.P. Martin¹⁸, G. Martinez¹⁷, T. Mashimo²⁴, P. Mättig²⁶, W.J. McDonald³⁰, J. McKenna²⁹,
 E.A. Mckigney¹⁵, T.J. McMahon¹, R.A. McPherson²⁸, F. Meijers⁸, S. Menke³, F.S. Merritt⁹,
 H. Mes⁷, J. Meyer²⁷, A. Michelini², S. Mihara²⁴, G. Mikenberg²⁶, D.J. Miller¹⁵, R. Mir²⁶,
 W. Mohr¹⁰, A. Montanari², T. Mori²⁴, K. Nagai⁸, I. Nakamura²⁴, H.A. Neal¹², R. Nisius⁸,
 S.W. O’Neale¹, F.G. Oakham⁷, F. Odorici², H.O. Ogren¹², M.J. Oreglia⁹, S. Orito²⁴,
 J. Pálinkás^{33,d}, G. Pásztor³², J.R. Pater¹⁶, G.N. Patrick²⁰, J. Patt¹⁰, R. Perez-Ochoa⁸,
 S. Petzold²⁷, P. Pfeifenschneider¹⁴, J.E. Pilcher⁹, J. Pinfold³⁰, D.E. Plane⁸, P. Poffenberger²⁸,
 B. Poli², J. Polok⁸, M. Przybycień^{8,f}, C. Rembser⁸, H. Rick⁸, S. Robertson²⁸, S.A. Robins²²,
 N. Rodning³⁰, J.M. Roney²⁸, S. Rosati³, K. Roscoe¹⁶, A.M. Rossi², Y. Rozen²², K. Runge¹⁰,
 O. Runolfsson⁸, D.R. Rust¹², K. Sachs¹⁰, T. Saeki²⁴, O. Sahr³⁴, W.M. Sang²⁵,
 E.K.G. Sarkisyan²³, C. Sbarra²⁹, A.D. Schaile³⁴, O. Schaile³⁴, P. Scharff-Hansen⁸, J. Schieck¹¹,
 S. Schmitt¹¹, A. Schöning⁸, M. Schröder⁸, M. Schumacher³, C. Schwick⁸, W.G. Scott²⁰,
 R. Seuster¹⁴, T.G. Shears⁸, B.C. Shen⁴, C.H. Shepherd-Themistocleous⁸, P. Sherwood¹⁵,
 G.P. Siroli², A. Sittler²⁷, A. Skuja¹⁷, A.M. Smith⁸, G.A. Snow¹⁷, R. Sobie²⁸,
 S. Söldner-Rembold¹⁰, S. Spagnolo²⁰, M. Sproston²⁰, A. Stahl³, K. Stephens¹⁶, J. Steuerer²⁷,

K. Stoll¹⁰, D. Strom¹⁹, R. Ströhmer³⁴, B. Surov⁸, S.D. Talbot¹, P. Taras¹⁸, S. Tarem²²,
R. Teuscher⁸, M. Thiergen¹⁰, J. Thomas¹⁵, M.A. Thomson⁸, E. Torrence⁸, S. Towers⁶,
I. Trigger¹⁸, Z. Trócsányi³³, E. Tsur²³, A.S. Turcot⁹, M.F. Turner-Watson¹, I. Ueda²⁴,
R. Van Kooten¹², P. Vannerem¹⁰, M. Verzocchi¹⁰, H. Voss³, F. Wäckerle¹⁰, A. Wagner²⁷,
C.P. Ward⁵, D.R. Ward⁵, P.M. Watkins¹, A.T. Watson¹, N.K. Watson¹, P.S. Wells⁸,
N. Wermes³, J.S. White⁶, G.W. Wilson¹⁶, J.A. Wilson¹, T.R. Wyatt¹⁶, S. Yamashita²⁴,
G. Yekutieli²⁶, V. Zacek¹⁸, D. Zer-Zion⁸

¹School of Physics and Astronomy, University of Birmingham, Birmingham B15 2TT, UK

²Dipartimento di Fisica dell' Università di Bologna and INFN, I-40126 Bologna, Italy

³Physikalisches Institut, Universität Bonn, D-53115 Bonn, Germany

⁴Department of Physics, University of California, Riverside CA 92521, USA

⁵Cavendish Laboratory, Cambridge CB3 0HE, UK

⁶Ottawa-Carleton Institute for Physics, Department of Physics, Carleton University, Ottawa, Ontario K1S 5B6, Canada

⁷Centre for Research in Particle Physics, Carleton University, Ottawa, Ontario K1S 5B6, Canada

⁸CERN, European Organisation for Particle Physics, CH-1211 Geneva 23, Switzerland

⁹Enrico Fermi Institute and Department of Physics, University of Chicago, Chicago IL 60637, USA

¹⁰Fakultät für Physik, Albert Ludwigs Universität, D-79104 Freiburg, Germany

¹¹Physikalisches Institut, Universität Heidelberg, D-69120 Heidelberg, Germany

¹²Indiana University, Department of Physics, Swain Hall West 117, Bloomington IN 47405, USA

¹³Queen Mary and Westfield College, University of London, London E1 4NS, UK

¹⁴Technische Hochschule Aachen, III Physikalisches Institut, Sommerfeldstrasse 26-28, D-52056 Aachen, Germany

¹⁵University College London, London WC1E 6BT, UK

¹⁶Department of Physics, Schuster Laboratory, The University, Manchester M13 9PL, UK

¹⁷Department of Physics, University of Maryland, College Park, MD 20742, USA

¹⁸Laboratoire de Physique Nucléaire, Université de Montréal, Montréal, Quebec H3C 3J7, Canada

¹⁹University of Oregon, Department of Physics, Eugene OR 97403, USA

²⁰CLRC Rutherford Appleton Laboratory, Chilton, Didcot, Oxfordshire OX11 0QX, UK

²²Department of Physics, Technion-Israel Institute of Technology, Haifa 32000, Israel

²³Department of Physics and Astronomy, Tel Aviv University, Tel Aviv 69978, Israel

²⁴International Centre for Elementary Particle Physics and Department of Physics, University of Tokyo, Tokyo 113-0033, and Kobe University, Kobe 657-8501, Japan

²⁵Institute of Physical and Environmental Sciences, Brunel University, Uxbridge, Middlesex UB8 3PH, UK

²⁶Particle Physics Department, Weizmann Institute of Science, Rehovot 76100, Israel

²⁷Universität Hamburg/DESY, II Institut für Experimental Physik, Notkestrasse 85, D-22607 Hamburg, Germany

²⁸University of Victoria, Department of Physics, P O Box 3055, Victoria BC V8W 3P6, Canada

²⁹University of British Columbia, Department of Physics, Vancouver BC V6T 1Z1, Canada

³⁰University of Alberta, Department of Physics, Edmonton AB T6G 2J1, Canada

³¹Duke University, Dept of Physics, Durham, NC 27708-0305, USA

³²Research Institute for Particle and Nuclear Physics, H-1525 Budapest, P O Box 49, Hungary

³³Institute of Nuclear Research, H-4001 Debrecen, P O Box 51, Hungary

³⁴Ludwigs-Maximilians-Universität München, Sektion Physik, Am Coulombwall 1, D-85748 Garching, Germany

^a and at TRIUMF, Vancouver, Canada V6T 2A3

^b and Royal Society University Research Fellow

^c and Institute of Nuclear Research, Debrecen, Hungary

^d and Department of Experimental Physics, Lajos Kossuth University, Debrecen, Hungary

^e on leave of absence from the University of Freiburg

^f and University of Mining and Metallurgy, Cracow

1 Introduction

Particle density fluctuations of hadronic final states produced in high-energy collisions have been extensively investigated in the last decade. For recent reviews, see *e.g.* Refs. [1, 2]. Dynamical (*i.e.*, non-statistical) fluctuations were observed, establishing the phenomenon of intermittency, the increase of factorial moments with decreasing bin size [3]. The intermittency approach of studying the distributions of particles in restricted regions of phase space allows a detailed analysis of the dynamics of hadroproduction. Furthermore, the behaviour of the factorial moments shows the self-similar nature of density fluctuations, *i.e.*, the particle distributions show similar fluctuations on all resolution scales, a characteristic of fractals [4].

Despite numerous experimental and theoretical studies, the origin of intermittency remains unclear, although important features of this effect have been observed [2]. For example, experimental investigations have shown an enhancement of the phenomenon in e^+e^- annihilation as compared to hadronic and nuclear collisions. Furthermore, larger intermittency effects have been observed when several dynamical variables are considered together, as compared to the effect seen in one-dimensional analyses. Existing Monte Carlo (MC) models, which use parton shower simulations and differing fragmentation and hadronization models, simulate most details of e^+e^- collisions and the general properties of hadronic interactions well, but fall short in predicting the intermittent structure found in the data, both in e^+e^- collisions and in hadronic interactions. Theoretical approaches have not clarified the origin of the observed dynamical fluctuations. The intermittent behaviour of particle distributions may prove to be a strong test of QCD, which already provides guidelines for explaining the “soft” character of intermittency [5, 6].

The goal of this study is to investigate the dynamical correlations of many-particle systems produced in e^+e^- annihilation. One must be careful to separate out the effects of lower-order correlations when searching for higher-order ones. For example, a correlation in the production of pairs of particles in neighboring regions of phase space will necessarily induce correlations when particles are considered three at a time. It has been suggested that intermittency should therefore be analysed in terms of the factorial cumulant moments to reveal “genuine” multiparticle correlations by not being sensitive to the contributions of lower-order correlations [7]. The investigations carried out for heavy-ion reactions have not shown any correlations higher than two-particle ones, while in studies of hadron-hadron collisions significant higher-order correlations have been observed, although the latter have been seen to weaken with increasing multiplicity at a fixed centre-of-mass energy [2]. These effects have been explained as a consequence of the events consisting of superpositions of multiple independent particle sources [8]. These findings suggest that interactions with a low number of very hard scattering processes, such as high-energy e^+e^- annihilation, might be more sensitive to genuine multiparticle correlations.

This paper describes the study of the intermittency phenomena and the genuine multiparticle correlations of charged particles in the three-dimensional phase space of rapidity, transverse momentum, and azimuthal angle, as defined in Section 3. This analysis uses more than four million multihadronic events recorded by the OPAL detector at the LEP collider with $\sqrt{s} \approx m_{Z^0}$.

This data sample is much larger than that used in OPAL’s previous publication [9], and in other e^+e^- investigations carried out at the Z^0 peak [10–14] and at lower energies [13, 15]. The statistical precision of this data sample allows us to extend the former intermittency analysis [9] to a multidimensional one with the possibility to reach high-order fluctuations at very small bins. With this high statistics we are able for the first time to search for genuine multiparticle correlations by means of normalized factorial cumulants in e^+e^- collisions.

The paper is organised as follows. In Section 2 the normalized factorial moments and factorial cumulant moments are introduced and the technique of extracting dynamical fluctuations and genuine multiparticle correlations is given. The detector, data sample and correction procedure are described in Section 3. The results and their comparison with MC predictions are presented and discussed in Section 4. In Section 5 both a summary and conclusions are presented.

2 The method

2.1 Scaled factorial moments and intermittency

To search for local dynamical fluctuations we use the normalized scaled factorial moments introduced in Ref. [3]. The moments are defined as

$$F_q = \mathcal{N}^q \left\langle \overline{n_m^{[q]}} \right\rangle / \bar{N}_m^{[q]}. \quad (1)$$

Here $n_m^{[q]}$ is the q th order factorial multinomial, $n_m(n_m - 1) \cdots (n_m - q + 1)$, with n_m particles in the m th bin of the phase space (e.g. rapidity interval) divided into M equal bins. N_m is the number of particles in the m th bin summed over all the \mathcal{N} events in the sample, $N_m = \sum_{j=1}^{\mathcal{N}} (n_m)_j$. The bar indicates averaging over the bins in each event, $(1/M) \sum_{m=1}^M$ (“horizontal” averaging), while the angle brackets denote averaging over the events (“vertical” averaging).

The moments in Eq. (1) are given in the modified form, in contrast to those used in the earlier e^+e^- studies [9–15]. This form has been suggested in Ref. [16] to take into account the bias arising from the assumption of infinite statistics in the normalization calculation [3, 17] and affects the moments, particularly those computed with small bins.

These moments, defined in Eq. (1), are the so-called “horizontal” moments [17], where the fluctuations are first averaged over all M bins in each event and then the average over all events is taken.¹ These moments are determined for a flat-shape single-particle distribution. In order to account for non-flatness, we apply the correction procedure proposed in Refs. [17, 19], so that the corrected modified factorial moments [16] are given in the reduced form,

$$F_q^C = F_q / R_q, \quad R_q = \overline{N_m^{[q]}} / \bar{N}_m^{[q]}, \quad (2)$$

¹ For a survey of types of factorial moments see Ref. [18].

where R_q is the correction factor, and it is equal to unity for a flat single-particle distribution.

The non-statistical fluctuations have been shown [3] to lead to increasing factorial moments with increasing number (decreasing size) of the phase-space regions, or bins. Such an increase, expressed as a scaling law,

$$F_q(M) \propto M^{\varphi_q} \quad (M \rightarrow \infty), \quad 0 < \varphi_q \leq q - 1, \quad (3)$$

indicates the presence of self-similar dynamics. This increase is called intermittency and the powers φ_q , or intermittency slopes, show the strength of the effect. The size of the smallest bin under investigation is limited by the characteristic correlation length (saturation effect) and/or by the apparatus resolution [3]. In practice, saturation happens much earlier because of statistical limitations (the “empty bin effect” [20]), which we here attempt to reduce by using the modified moments. Therefore, in the following we use the term “intermittency” to refer only to the rise of the factorial moments with decreasing bin size.

2.2 Factorial cumulant moments and genuine multiparticle correlations

To extract the genuine multiparticle correlations, the technique of normalized factorial cumulant moments, or cumulants, K_q , proposed in Ref. [7], is used. The cumulants are constructed from the q -particle cumulant correlation functions which vanish whenever one of their arguments becomes independent of the others, so that they measure the genuine correlations. The factorial cumulants remove the influence of the statistical component of the correlations in the same way as the factorial moments.

Similarly to the factorial moments, we use the corrected modified cumulants, defined as

$$K_q^C = \mathcal{N}^q \bar{k}_q^{(m)} / \overline{N_m^{[q]}}. \quad (4)$$

The normalization factor, $\overline{N_m^{[q]}}$ (instead of $\bar{N}_m^{[q]}$), comes from the correction procedure expressed in Eq. (2) and takes into account the non-flat shape of the single-particle distribution. The $k_q^{(m)}$ factors are the unnormalized factorial cumulant moments or the Mueller moments [21], and represent genuine q -particle correlations where the lower-order contributions are eliminated by subtracting the appropriate combinations of the unnormalized factorial moments, $\langle n_m^{[p]} \rangle$, of order $p < q$ from the q th order one, *e.g.*

$$k_3^{(m)} = \langle n_m^{[3]} \rangle - 3 \langle n_m^{[2]} \rangle \langle n_m \rangle + 2 \langle n_m \rangle^3. \quad (5)$$

In order to find contributions from genuine multiparticle correlations to the factorial moments we use the relations between the moments and the cumulants [22],

$$\begin{aligned}
F_2 &= K_2 + 1, \\
F_3 &= K_3 + 3K_2 + 1, \\
F_4 &= K_4 + 4K_3 + 3\overline{(K_2^{(m)})^2} + 6K_2 + 1, \\
F_5 &= K_5 + 5K_4 + 10\overline{K_3^{(m)}K_2^{(m)}} + 10K_3 + 15\overline{(K_2^{(m)})^2} + 10K_2 + 1, \text{ etc.}
\end{aligned}
\tag{6}$$

with $K_q^{(m)} = k_q^{(m)} / \langle n_m \rangle^q$. Here and below in this section, for brevity we omit the superscript C . These relations are exact for the “vertical” moments and cumulants and the errors introduced by using them with corrected horizontal moments and cumulants are negligibly small, except when very high orders are considered for variables whose single-particle distributions are markedly non-uniform [2].

The composition of the q -particle dynamical fluctuations from the genuine lower-order p -particle correlations is tested by the comparison of the q th order factorial moments with the p -particle contribution $F_q^{(p)}$ calculated by the above Eqs. (6), which are truncated up to the K_p -terms. The excess of F_q over $F_q^{(p)}$ demonstrates the importance of correlations of order higher than p in the measured q -particle fluctuations.

For example, the two-particle contribution $F_4^{(2)}$ to the fourth-order factorial moment can be expressed as

$$F_4^{(2)} = \overline{(K_2^{(m)})^2} + 6K_2 + 1, \tag{7}$$

while the contribution from two and three-particle correlations, $F_4^{(2+3)}$, is

$$F_4^{(2+3)} = 4K_3 + 3\overline{(K_2^{(m)})^2} + 6K_2 + 1. \tag{8}$$

3 Experimental details

The data used in this study were recorded with the OPAL detector [23] at the LEP e^+e^- collider at CERN. The analysis is restricted to charged particles measured in the central tracking chambers. The inner vertex detector has a high precision in impact parameter reconstruction. The large diameter jet chamber and outer layer of longitudinal drift chambers allow accurate measurements in the planes perpendicular and parallel to the beam axis. The jet chamber provides up to 159 space points per track, and allows particle identification by measuring the ionisation energy loss, dE/dx , of charged particles [24]. All tracking chambers are surrounded by a solenoidal coil providing a magnetic field of 0.435 T along the beam axis. The resolution of the component of momentum perpendicular to the beam axis is $\sigma(p_t)/p_t = \sqrt{(0.0023p_t)^2 + (0.018)^2}$ for p_t in GeV/ c , and the resolution in the angle θ between the charged particle’s direction and the electron beam is $\sigma(\theta) = 5$ mrad within the acceptance of the analysis presented here. In multihadronic events, the ionisation energy loss measurement has been obtained with a resolution of $\simeq 3.5\%$ for tracks with 159 measured points.

The present study was performed with a sample of approximately 4.1×10^6 hadronic Z^0 decays collected from 1991 through 1995. About 96% of this sample was collected at the Z^0 peak energy and the remaining part was collected within ± 3 GeV of the peak. Over 98% of charged hadrons were detected.

The event selection criteria are based on the multihadronic event selection algorithms described in Refs. [9,25], and are similar to those used in other LEP intermittency studies [10–12].

For each event, “good” charged tracks were accepted if they

- had at least 20 measured points in the jet chamber;
- had a first measured point closer than 70 cm from the beam axis;
- pass within 5 cm of the e^+e^- collision point in the projection perpendicular to the beam axis, with the corresponding distance along the beam axis not exceeding 40 cm;
- had a momentum component transverse to the beam direction greater than 0.15 GeV/ c ;
- had a momentum smaller than 10 GeV/ c ;
- had a measured polar angle of the track with respect to the beam direction satisfying $|\cos \theta| < 0.93$;
- had a mean energy loss, dE/dx , in the jet chamber smaller than 9 keV/cm to reject electrons and positrons.

Selected multihadron events were required to have

- at least 5 good tracks;
- a momentum imbalance of $< 0.4\sqrt{s}$, which is defined as the magnitude of the vector sum of the momenta of all charged particles;
- the sum of the energies of all tracks (assumed to be pions) greater than $0.2\sqrt{s}$;
- $|\cos \theta_S| < 0.7$, where θ_S is the polar angle of the event sphericity axis with respect to the beam direction. The sphericity axis is calculated using all good tracks and electromagnetic and hadronic calorimeter clusters.

The first three requirements provide rejection of background from non-hadronic Z^0 decays, two-photon events, beam-wall interactions, and beam-gas scattering. The last requirement ensures that the event is well contained in the most sensitive volume of the detector. A total of about 2.3×10^6 events were selected for further analysis.

We also used two samples of about 2×10^6 simulated events each, generated at Z^0 peak energy using the following MC generators:

- JETSET version 7.4 [26] with the parton shower followed by string formation and fragmentation,
- HERWIG version 5.9 [27] with the parton shower followed by cluster fragmentation.

The parameters of both MC codes were tuned with OPAL data [28] to provide a good description of the distributions of the measured event-shape variables and single-particle kinematic variables.

In this study we chose rapidity, azimuthal angle and transverse momentum as individual track kinematic variables. These are frequently used in multihadronic studies [29] and, in particular, for intermittency and correlation analyses [1, 2, 5, 6, 30]. To make our study compatible with other investigations carried out in e^+e^- annihilations, these variables are calculated with respect to the sphericity axis as follows:

- Rapidity, $y = 0.5 \ln[(E + p_{\parallel})/(E - p_{\parallel})]$ with E and p_{\parallel} being the energy (assuming the pion mass) and longitudinal momentum of the particle in the interval $-2.0 \leq y \leq 2.0$.
- Transverse momentum in the interval $-2.4 \leq \ln(p_T) \leq 0.7$. The log scale is introduced, since the exponential shape of the p_T -distribution causes instability in the average multiplicity calculations, even for p_T bins of intermediate size.
- Azimuthal angle, Φ , calculated with respect to the eigenvector of the momentum tensor having the smallest eigenvalue, in the plane perpendicular to the sphericity axis. The angle Φ is defined in the interval $0 \leq \Phi \leq 2\pi$.

The single-particle distributions of the data sample and of the MC (corrected to the hadron level, see below) are shown in Fig. 1. In the following study the maximum number of bins is taken to be $M_{\max}=400$, so that the one-dimensional minimal bin size of the above kinematic variables are: $\delta y_{\min}=0.01$, $\delta\Phi_{\min}=0.9^\circ$ and $\delta(\ln p_T)_{\min}\simeq 0.008$. M_{\max} is the same as was chosen in our previous intermittency publication [9] and is the largest value of M used so far. The experimental resolution of each variable was estimated by a MC simulation. It was found that the OPAL detector allows the study of an intermittency signal down to distances of the above mentioned minimal bin sizes, although detector effects become important for bin sizes less than 0.04 in rapidity, smaller than 3° in azimuthal angle and less than 0.02 in $\ln p_T$. The distributions in several dimensions have the advantage that the event phase space may be subdivided into many more bins than M_{\max} before the limits of detector resolution are reached. As in our former analysis, the smallest bin sizes used are found not to affect the observations.

To correct the measured moments for the effects of geometrical acceptance, kinematic cuts, initial-state radiation, resolution and particle decays, we apply the correction procedure adopted in our earlier factorial moment study [9] and in analogous investigations done with e^+e^- annihilation [10–14]. Two samples of multihadronic events were generated using the JETSET 7.4 MC program. The first sample does not include the effects of initial-state radiation, and all particles with lifetimes longer than 3×10^{-10} seconds were regarded as stable. The generator-level factorial moments and cumulants are calculated directly from the charged particle distributions of this sample without any selection criteria. The second sample was generated including the

effects of finite lifetimes and initial-state radiation and was passed through a full simulation of the OPAL detector [31]. The corresponding detector-level moments were calculated from this set using the same reconstruction and selection algorithms as used for the measured data. The corrected moments were then determined by multiplying the measured ones by the factor

$$U_q(M) = X_q(M)_{gen}/X_q(M)_{det} , \quad (9)$$

with $X_q = F_q^C$ or K_q^C defined by Eqs. (2) and (4).

The correction factors U_q have also been computed using the HERWIG event sample. For both JETSET and HERWIG MC generators, the correction factor tends to be less than unity and rises with order q as has been observed earlier [9, 10, 12]. The difference between the X_q quantities calculated with the JETSET and HERWIG generated samples has been used in the estimation of the systematic uncertainties. The statistical uncertainties on the JETSET U_q factor have been also incorporated into the systematic uncertainties in this analysis.

Another contribution to the systematic uncertainties has been evaluated by changing the above track and event selection criteria. The moments have been calculated from the data sample of about two million events with the following variations in the selection criteria: the first measured point was required to be closer than 40 cm to the beam axis, the requirement of the transverse momentum with respect to the beam axis was removed, the total momentum was required to be less than 40 GeV/ c , the charged track polar angle acceptance was changed to $|\cos\theta| < 0.7$, and the requirement on the mean energy loss was removed. The deviations of the moments with these changes modify the results by no more than a few percent and do not influence their behaviour.

The total errors have been calculated by adding the systematic and statistical uncertainties in quadrature. The systematic uncertainties are shown separately in the figures (except in those given in Section 4.3) and are dominant at large M . Statistical uncertainties based on the MC samples are similar to those obtained from the data.

It was verified that the results do not appreciably change if one removes from the analysis those events which were taken at energies off the Z^0 peak energy.

4 Results and discussion

4.1 The measurements

In this section we present the factorial moments F_q^C and the cumulants K_q^C , defined in Eqs. (2) and (4), respectively, and compute them in the $y \times \Phi \times p_T$ phase space and its projections. The moments are shown in Figs. 2 to 4 and the cumulants are given in Figs. 5 to 7 as a function of M , the number of bins in one, two and three dimensions. Both the factorial moments and the cumulants are measured up to the fifth order. The second-order cumulants are not shown since their behaviour is determined directly by the second-order factorial moments, as can be seen from Eqs. (6). The higher-order cumulants behave differently from the same-order moments

because the cumulants contain combinations of lower-order fluctuations, which are taken into account in Eq. (4) by means of the Mueller moments as in Eq. (5).

Overall, the factorial moments and the cumulants depend very similarly on the bin width. The factorial moments obey the scaling-law of Eq. (3) in almost all the phase-space projections (except in the p_T -subspace), and the cumulants show analogous intermittent behaviour up to high orders. This behaviour becomes more pronounced when the analysis is extended to several dimensions where, in contrast to the one-dimensional case, no saturation with decreasing bin size is observed. The largest moments and cumulants and the largest intermittency slopes are found in the $y \times \Phi$ subspace.

The saturation at small bin sizes observed in the one-dimensional analysis in rapidity and azimuthal angle (Figs. 2 and 5) agrees with that predicted by QCD [5] and is a consequence of the transition to the regime where the running of the QCD coupling α_s comes into play. The dynamics governing particle density fluctuations in small bins occurs at low energy scales with larger values of α_s . One can see that the moments and the cumulants actually have steep linear rises at $M \lesssim 20$ ($\delta y \gtrsim 0.2$, $\delta \Phi \gtrsim 18^\circ$) and level off at large values of M . Figs. 2 and 5 show that the transition point shifts to larger M (smaller bin sizes) as the order q of the moments increases, also in accordance with QCD calculations.

The enhancement of the intermittency effect in higher dimensions as shown in Figs. 3 and 4 for the factorial moments and in Figs. 6 and 7 for the cumulants, has been attributed to “shadowing” *i.e.*, studies in lower dimensions lose information due to projection [32, 33]. A model of emission of strongly collimated particles, clustered in both rapidity and azimuth, has been suggested in [32]. In the framework of this so-called “pencil-jet” model, a strong increase of the factorial moments is expected in the $y \times \Phi$ subspace compared to y or Φ separately. Although formation of such jet structures has been confirmed experimentally, the increase has been found to be much less than that predicted [2].

Jet structure also explains the behaviour observed in the $y \times p_T$ and $\Phi \times p_T$ plots of Figs. 3 and 6. Indeed, the moments and the cumulants in $y \times p_T$ and $\Phi \times p_T$ for the same total M are not found to increase as compared to those in y and Φ , respectively, since there is no intermittency in the transverse momentum subspace. Similarly, the moments in $y \times \Phi$ are approximately equal to those in $y \times \Phi \times p_T$ at the same total M . At the same time, the intermittency is seen for larger M in higher dimensions, indicating the presence of the dynamical fluctuations and correlations in additional dimensions.

In Ref. [30] it was claimed that the increase of the factorial moments with the addition of new dimensions is a trivial consequence of a phase-space factor and has nothing to do with the jet formation mechanism. Our observations show that this is true if one compares the moments at the same abscissa $M^{1/d}$, where d is the dimension of the subspace. However, comparing multidimensional moments (and the cumulants) at the same *total* number of bins, one obtains contributions of self-similar structure from different projections, as is the case with the jet-structure contributions to the $y \times \Phi$ moments.

The values of the cumulants are positive in most of the cases, indicating that multiparticle dynamical correlations indeed are significantly present in the particle-production process. Large values of the cumulants of the order $q \geq 4$ are seen in $y \times \Phi$ and $y \times \Phi \times p_T$. Non-zero high-order cumulants are also found in rapidity and $y \times p_T$. This shows that the factorial moments at $q=5$, the highest order considered here, have important contributions from lower-order correlations, a point discussed in Section 4.3.

4.2 Comparison with the Monte Carlo models

In Figs. 2 through 7 the data are compared with the predictions of the JETSET and HERWIG MC models. Both MC models describe the general behaviour of the factorial moments and cumulants and show significant positive multiparticle correlations.

The one-dimensional factorial moments (Fig. 2) and cumulants (Fig. 5) in rapidity and in azimuthal angle show that while the MC describe the data rather well at small M (large bin sizes), the models tend to fall below the data, starting at intermediate M . The discrepancy rises with M and with the order of the moments q . The saturation effect sets in earlier in the MC models than it does in the data. In the transverse momentum projection, the models show quite different behaviour. JETSET underestimates the moments and the cumulants, whereas HERWIG strongly overestimates them. Figs. 3, 4, 6 and 7 show that there is a better agreement between the data and the MC in high dimensions.

From these comparisons one can conclude that both MC models reproduce the data well while neither of them is particularly preferred. The perturbative parton shower, on which both MC models are based, seems to play an important role in the origin of the dynamical fluctuations and correlations in e^+e^- annihilation. The observed differences between the two MC descriptions indicate that the last steps of the hadronization process are not described correctly [2]. Contributions from additional mechanisms to the observed fluctuations and correlations are not excluded.

4.3 Contributions from multiparticle correlations

This section describes the contributions of genuine multiparticle correlations to dynamical fluctuations. To this end we compare in Figs. 8–12 the measured corrected factorial moments to the lower-order contributions, $F_q^{C(p)}$, calculated using Eqs. (6).

Fig. 8 shows the one-dimensional case. The fluctuations in transverse momentum are not shown since they do not exhibit intermittency behaviour (see Fig. 2). A significant contribution of high-order genuine correlations appears. Two-particle correlations in rapidity and in azimuthal angle are insufficient to explain the measured three-particle fluctuations. At $q=4$, four-particle correlations are also necessary. The importance of four-particle genuine correlations is also demonstrated by the five-particle fluctuations in the rapidity subspace, where the addition of the fourth-order cumulants becomes essential. The fifth-order moment study cannot be performed for the azimuthal angle variable because the non-uniformity of the Φ spectrum

leads to large values of the correction factor R_5 which makes the relations (6) inapplicable. The difference between the moments and the correlation contributions increases with decreasing bin size.

The genuine multiparticle contributions, also seen to be important in the two-dimensional $y \times \Phi$ analysis, are shown in Fig. 9. The failure of the genuine two- and three-particle correlations to describe the four-particle dynamical fluctuations indicates a significant four-particle contribution in the observed high-order fluctuations. The need to account for higher-order correlations is visible also in F_5 for small bin-sizes. The comparison of F_3^C and $F_3^{C(p)}$ for other two-dimensional subspaces, $y \times p_T$ and $\Phi \times p_T$, is shown in Figs. 10 and 11 and also indicates a considerable contribution from three-particle genuine correlations. As in the one-dimensional case in Φ , the large R_q factor for $q > 3$ does not allow use of Eqs. (6) in these cases. The same is seen in the three-dimensional study (Fig. 12) for $q=5$, whereas for $q < 5$, the contribution of multiparticle correlations up to the fourth order is well illustrated.

4.4 Comparison with other experiments

4.4.1 Factorial moments in e^+e^- annihilation

Studies of intermittency in e^+e^- interactions have been carried out mainly in one-dimension using the rapidity variable [2, 10–15]. The first three-dimensional analysis of factorial moments was performed by CELLO [15] in Lorentz-invariant phase space. DELPHI [10] has presented a three-dimensional analysis of intermittency in $y \times \Phi \times p_T$ phase space and its projections, as it is chosen in this paper. The values of the moments and their M -dependence, found in all these studies, are similar to those obtained here.

In one-dimensional rapidity and azimuthal angle the saturation of the factorial moments has been observed at the same M in all investigations [10–14]. The moments in two and three dimensions have been found [10] to be larger and to have steeper intermittency slopes than those in one dimension. Jet evolution has been suggested [9, 10, 34] as the main source of multiparticle fluctuations, similarly to our finding. However, the saturation shown by DELPHI for the two-dimensional factorial moments are not present in our analysis due to the high statistics and the modification used to take into account the contents of small bins.

In agreement with recent e^+e^- studies [10–12, 14], the MC models used here are found to describe the behaviour of the measured moments, although they underestimate their magnitudes.

4.4.2 Factorial moments and cumulants in hadronic collisions

The factorial moments have also been investigated in $y \times \Phi \times p_T$ phase space and in its projections in hadron-hadron collisions by NA22 [35].

In the NA22 p_T -subspace analysis, hadronic interactions have shown a visible intermittency effect, in contrast to its absence in e^+e^- annihilation. In Φ , on the other hand, one finds sensi-

tive dynamical fluctuations in e^+e^- collisions, while in hadronic collisions the fluctuations are strongly suppressed by a statistical component. No saturation has been observed in y and p_T subspaces in hadronic collisions.

In several dimensions the factorial moments computed in hadronic interactions also differ from those in e^+e^- annihilation. In two-dimensions, the largest moments are found to be in $y \times p_T$, and the intermittency effect is observed to be the strongest in $y \times \Phi$. These moments show a faster increase (larger φ_q) than those in one dimension, although their values are lower and saturate already at $q=3$. The three-dimensional moments show strong increase with decreasing bin size, although their values are found to be closer to the two-dimensional moments. In contrast to the linear log-log plots of the scaling behaviour (3) observed in e^+e^- annihilation, three-dimensional factorial moments in hadronic collisions scale only approximately; they rise more quickly than the power law of Eq. (3). This difference is attributed to the difference in dynamics between soft and hard processes that leads to isotropic dynamical fluctuations in e^+e^- annihilation and to anisotropic ones in hadron-hadron collisions [36].

Large cumulant values are expected in e^+e^- annihilation due to a small number of very energetic particle sources, as was mentioned in the introduction. Indeed, the cumulants measured here are much higher than those found in hadronic interactions. Furthermore, they have non-zero values for higher orders, while in hadronic collisions they are consistent with zero at $q>3$. Also, the power-law increase in M is seen to be stronger in the present data.

In hadronic interactions [2], both in one [22] and several dimensions [35], the factorial moments were found to be basically composed of two-particle correlations. Our study shows sensitive contributions of correlations of orders $q=3$ and even 4 to the dynamical fluctuations in e^+e^- annihilation. The observed contributions increase with decreasing bin size, in agreement with trends seen in hadronic interactions.

5 Summary and Conclusions

A multidimensional study of local fluctuations and genuine multiparticle correlations in hadronic decays of the Z^0 is carried out with the four-million event sample of the OPAL data collected at the LEP collider. The sphericity axis is chosen as a reference axis, and the phase space is defined by the rapidity, azimuthal angle and transverse momentum variables. The analysis is based on the intermittency approach and represents an investigation of the normalized factorial moments and, for the first time in e^+e^- annihilation, the normalized cumulants. The quantities studied have been corrected to reduce the bias due to the non-uniform shapes of the single-particle distributions and have been modified to eliminate effects of finite statistics. The factorial moments and cumulants are computed up to the fifth order and down to very small bin sizes.

The factorial moments show an intermittency behaviour which is strongly enhanced as the dimension of the subspace increases from one to three. In the one-dimensional analysis, the intermittency signal is found to be larger in rapidity than in azimuthal angle and to vanish in

transverse momentum. The moments in rapidity and in azimuthal angle saturate at intermediate bin sizes, in agreement with the QCD expectation for the transition to the running α_s coupling regime. No saturation is observed in two and three dimensions, a consequence of jet formation.

Our study of the cumulants shows that they have large positive values, indicating the existence of genuine multiparticle correlations. The cumulants are found to be much larger than those in hadronic interactions, suggesting an increase of the correlations with the decrease of the number of independent subprocesses present in the reaction. The cumulants are analysed in subspaces of different dimensions, and the genuine multiparticle correlations are found to be larger in higher dimensions. This study reveals genuine correlations up to four particles in one dimension and significant five-particle correlations in higher dimensions. Large higher-order correlations measured in the $y \times \Phi$ two-dimensional projection confirm the jet structure of dense groups of particles. The cumulants show intermittency rises which are stronger than for the corresponding factorial moments.

The large statistics of the present analysis allows the observation of contributions of many-particle correlations to the measured dynamical fluctuations. Considerable contributions up to four-particle are observed in the expansion of the factorial moments in terms of cumulants. The contributions increase with decreasing bin size reflecting the underlying self-similar dynamics.

The measurements are compared to HERWIG 5.9 and JETSET 7.4 predictions. In general, these Monte Carlo models are found to reproduce the behaviour of the moments and the cumulants, while underestimating the measured values starting at intermediate bin sizes. High-order multiparticle correlations are found to be present in both models used. The observations confirm jet structure formation as an important contribution to the correlations, but other mechanisms of the hadronization process are possibly also relevant.

Acknowledgements

We particularly wish to thank the SL Division for the efficient operation of the LEP accelerator at all energies and for their continuing close cooperation with our experimental group. We thank our colleagues from CEA, DAPNIA/SPP, CE-Saclay for their efforts over the years on the time-of-flight and trigger systems which we continue to use. In addition to the support staff at our own institutions we are pleased to acknowledge the
Department of Energy, USA,
National Science Foundation, USA,
Particle Physics and Astronomy Research Council, UK,
Natural Sciences and Engineering Research Council, Canada,
Israel Science Foundation, administered by the Israel Academy of Science and Humanities,
Minerva Gesellschaft,
Benozio Center for High Energy Physics,
Japanese Ministry of Education, Science and Culture (the Monbusho) and a grant under the

Monbusho International Science Research Program,
Japanese Society for the Promotion of Science (JSPS),
German Israeli Bi-national Science Foundation (GIF),
Bundesministerium für Bildung, Wissenschaft, Forschung und Technologie, Germany,
National Research Council of Canada,
Research Corporation, USA,
Hungarian Foundation for Scientific Research, OTKA T-016660, T023793 and OTKA F-023259.

References

- [1] P. Bożek, M. Płoszajczak and R. Botet, Phys. Reports **252** (1995) 101.
- [2] E.A. De Wolf, I.M. Dremin and W. Kittel, Phys. Reports **270** (1996) 1.
- [3] A. Białas and R. Peschanski, Nucl. Phys. **B 273** (1986) 703;
A. Białas and R. Peschanski, Nucl. Phys. **B 308** (1988) 857.
- [4] See e.g., G. Paladin and A. Vulpiani, Phys. Reports **156** (1987) 147.
- [5] Yu.L. Dokshitzer and I.M. Dremin, Nucl. Phys. **B 402** (1993) 139;
I.M. Dremin, Physics-Uspekhi **37** (1994) 715.
- [6] V.A. Khoze and W. Ochs, Int. J. Mod. Phys. **A 12** (1997) 2949.
- [7] P. Carruthers and I. Sarcevic, Phys. Rev. Lett. **63** (1989) 1562;
E.A. De Wolf, Acta Phys. Pol. **B 21** (1990) 611.
- [8] P. Lipa and B. Buschbeck, Phys. Lett. **B 223** (1989) 465.
- [9] OPAL Collaboration, M.Z. Akrawy *et al.*, Phys. Lett. **B 262** (1991) 351
- [10] DELPHI Collaboration, P. Abreu *et al.*, Phys. Lett. **B 247** (1990) 137;
DELPHI Collaboration, P. Abreu *et al.*, Nucl. Phys. **B 386** (1992) 471;
A. De Angelis, Mod. Phys. Lett. **A 5** (1990) 2395.
- [11] ALEPH Collaboration, D. Decamp *et al.*, Z. Phys. **C 53** (1992) 21;
ALEPH Collaboration, R. Barate *et al.*, Phys. Reports **294** (1997) 1.
- [12] L3 Collaboration, B. Adeva *et al.*, Z. Phys. **C 55** (1992) 39;
L3 Collaboration, M. Acciarri *et al.*, Phys. Lett. **B 429** (1998) 375;
S. Chekanov, Ph.D. Thesis, *Local Multiplicity Fluctuations and Intermittent Structure Inside Jets*, (Nijmegen Univ., 1997), unpublished.
- [13] W.N. Murray, Ph.D. Thesis, *Study of Intermittency in e^+e^- Collisions at $\sqrt{s} = 29$ GeV and 91 GeV*, report RX-1369 (Indiana Univ., 1991), unpublished.
- [14] J. Zhou (SLD Collaboration), Ph.D. Thesis, *Studies of Multiparticle Production in Hadronic Z^0 decays*, report SLAC-R-496 (1996), unpublished.
- [15] B. Buschbeck, P. Lipa, and R. Peschanski, Phys. Lett. **B 215** (1988) 788;
TASSO Collaboration, W. Braunschweig *et al.*, Phys. Lett. **B 231** (1989) 548;
CELLO Collaboration, H.-J. Behrend *et al.*, Phys. Lett. **B 256** (1991) 97.
- [16] K. Kadija and P. Seyboth, Z. Phys. **C 61** (1994) 465.
- [17] R. Peschanski, in: Proc. Santa-Fe Workshop on Intermittency in High-Energy Collisions (March 1990), F. Cooper, R.C. Hwa, and I. Sarcevic, eds. (World Scientific, 1991), p. 158.
- [18] M. Blažek, Int. J. Mod. Phys. **A 12** (1997) 839.

- [19] K. Fiałkowski, B. Wosiek, and J. Wosiek, *Acta Phys. Pol.* **B 20** (1989) 2651.
- [20] J.M. Alberty, R. Peschanski and A. Białas, *Z. Phys.* **C 52** (1991) 297;
P. Lipa *et al.*, *Z. Phys.* **C 54** (1992) 115;
M. Blažek, *Czech. J. Phys.* **43** (1993) 111.
- [21] M.G. Kendall and A. Stuart, *The Advanced Theory of Statistics* (C. Griffin & Co., London, 1969), Vol. 1;
A.H. Mueller, *Phys. Rev.* **D 4** (1971) 150.
- [22] P. Carruthers, H. Eggers and I. Sarcevic, *Phys. Lett.* **B 254** (1991) 258.
- [23] OPAL Collaboration, K. Ahmet *et al.*, *Nucl. Instr. Meth.* **A 305** (1991) 275;
P.P. Allport *et al.*, *Nucl. Instr. Meth.* **A 324** (1993) 34;
P.P. Allport *et al.*, *Nucl. Instr. Meth.* **A 346** (1994) 476.
- [24] M. Hauschild *et al.*, *Nucl. Instr. Meth.* **A 314** (1992) 74;
O. Biebel, *et al.*, *Nucl. Instr. Meth.* **A 323** (1992) 169.
- [25] OPAL Collaboration, P.D. Acton *et al.*, *Phys. Lett.* **B 267** (1991) 143;
OPAL Collaboration, P.D. Acton *et al.*, *Z. Phys.* **C 53** (1992) 539;
OPAL Collaboration, K. Ackerstaff *et al.*, *Eur. Phys. J.* **C 5** (1998) 239.
- [26] T. Sjöstrand, *Comp. Phys. Comm.* **82** (1994) 74.
- [27] G. Marchesini *et al.*, *Comp. Phys. Comm.* **67** (1992) 465.
- [28] OPAL Collaboration, G. Alexander *et al.*, *Z. Phys.* **C 69** (1996) 543.
- [29] T. Kanki *et al.*, *Prog. Theor. Phys. Suppl.* **97A** (1988) 1;
T. Kanki *et al.*, *Prog. Theor. Phys. Suppl.* **97B** (1989) 1.
- [30] I.V. Andreev *et al.*, *Int. J. Mod. Phys.* **A 10** (1995) 3951.
- [31] J. Allison *et al.*, *Nucl. Instr. Meth.* **A 317** (1992) 47.
- [32] W. Ochs and J. Wosiek, *Phys. Lett.* **B 214** (1988) 617.
- [33] W. Ochs, *Phys. Lett.* **B 247** (1990) 101; *Z. Phys.* **C 50** (1991) 339;
A. Białas and J. Seixas, *Phys. Lett.* **B 250** (1990) 161.
- [34] B. Buschbeck, in: *Proc. XXVth Int. Symp. on Multiparticle Dynamics* (Stará Lesná, 1995),
D. Bruncko, L. Šándor, and J. Urbán, eds. (World Scientific, 1996), p. 539.
- [35] EHS/NA22 Collaboration, N. Agababyan *et al.*, *Z. Phys.* **C 59** (1993) 405;
M. Charlet, Ph.D. Thesis, *Multiparticle Correlations in π^+p and K^+p interactions at 250 GeV/c*, (Nijmegen Univ., 1994), unpublished.
- [36] Liu Feng, Liu Fuming and Liu Lianshou, preprint HZPP-9808 (Huazhong Normal Univ., 1998), [hep-ph/9812309](#).

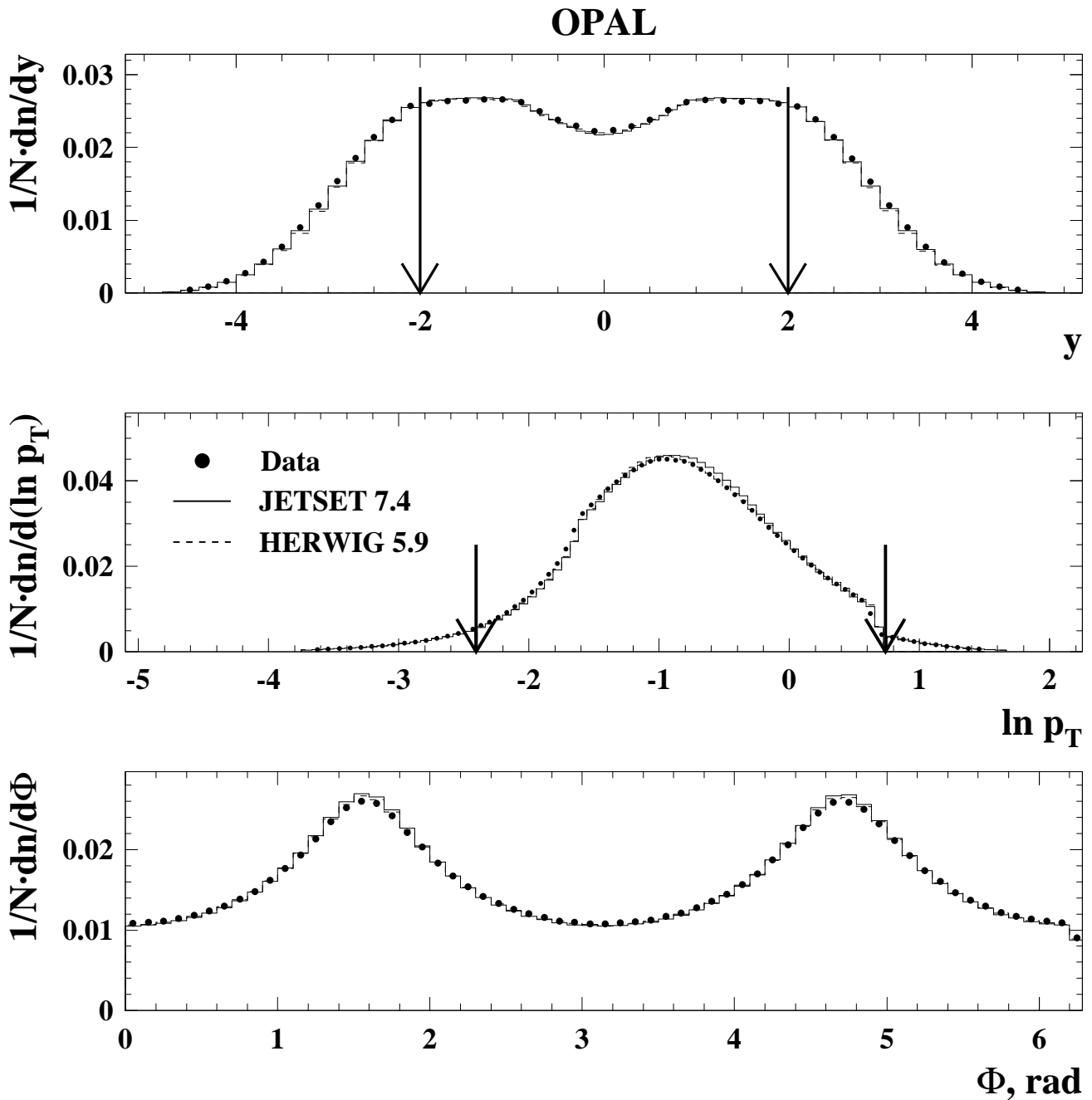


Figure 1: *The single-particle rapidity, the logarithm of the transverse momentum, and azimuthal angle distributions in the data and as predicted in two Monte Carlo models. All kinematic variables are calculated with respect to the sphericity axis. The distributions are corrected for detector effects in a bin-by-bin manner. The arrows show the intervals used in the analysis.*

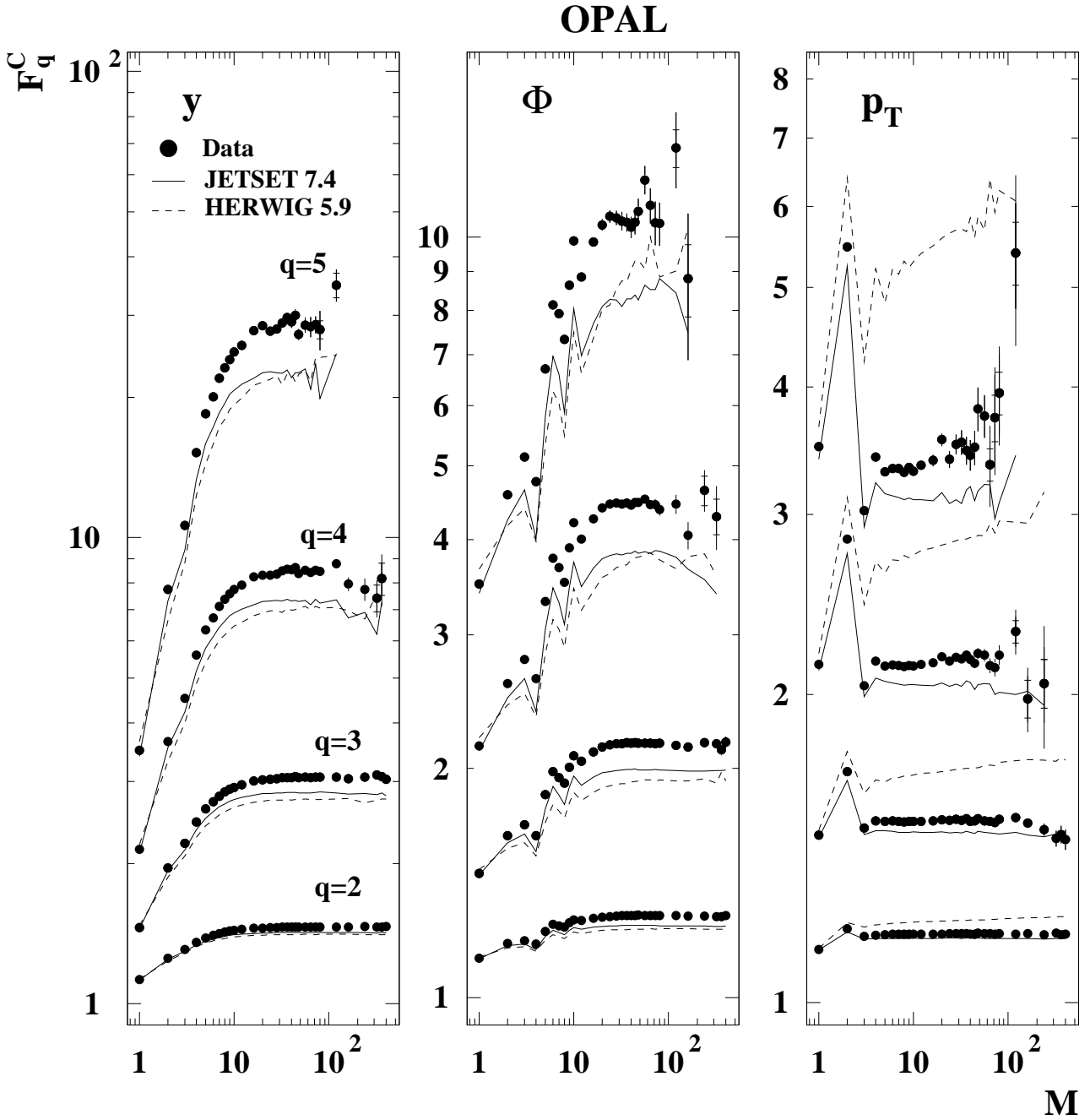


Figure 2: Factorial moments of order $q = 2$ to 5 vs. the number of bins M of the one-dimensional rapidity, azimuthal angle, and transverse momentum subspaces in comparison with the predictions of two Monte Carlo models. The total error is shown along with the statistical error (inner error bars) for each point.

OPAL

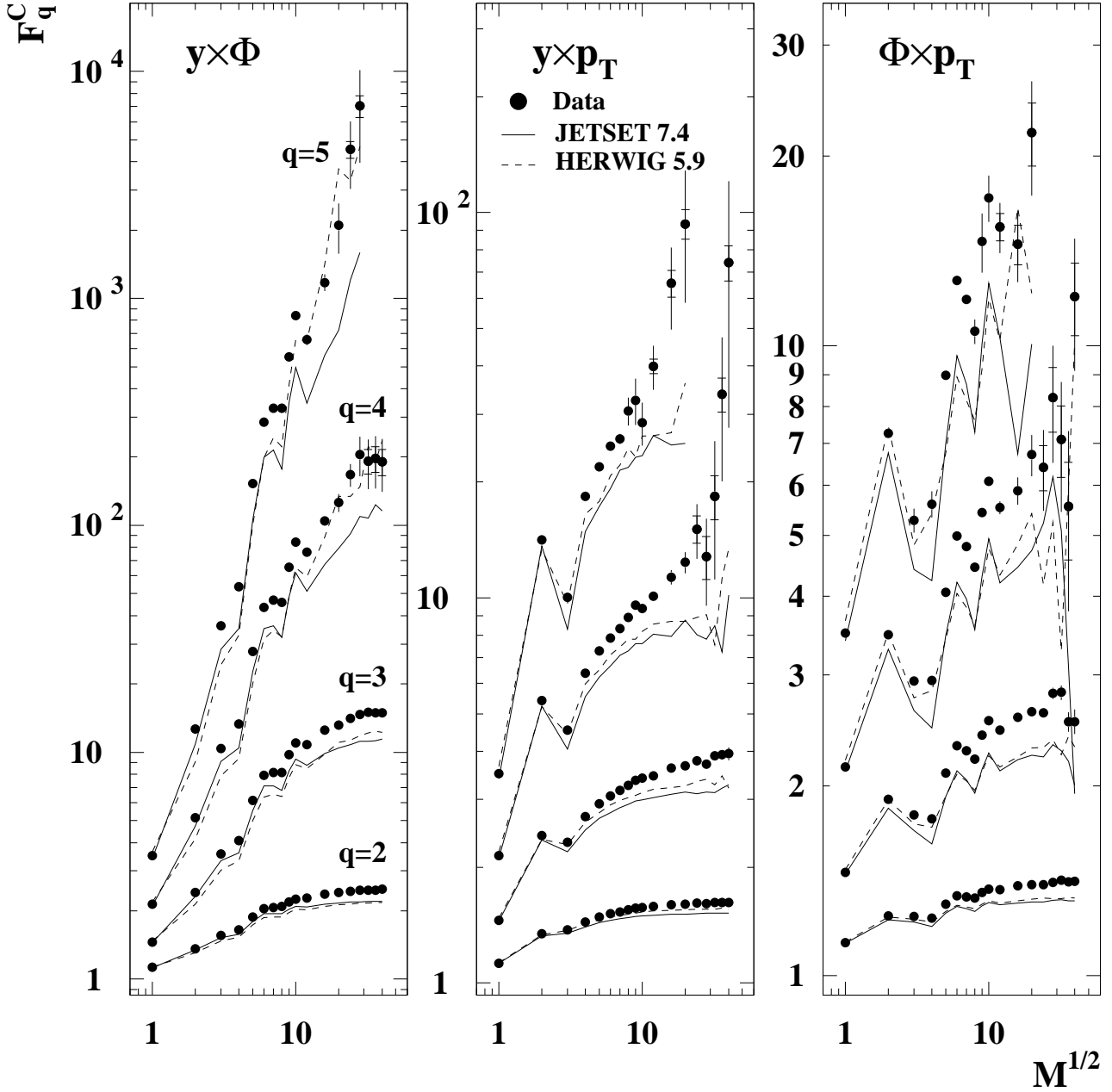


Figure 3: Factorial moments of order $q = 2$ to 5 vs. \sqrt{M} , where M is the number of bins of the two-dimensional subspaces of rapidity, azimuthal angle, and transverse momentum combinations, in comparison with the predictions of two Monte Carlo models. The total error is shown along with the statistical error (inner error bars) for each point.

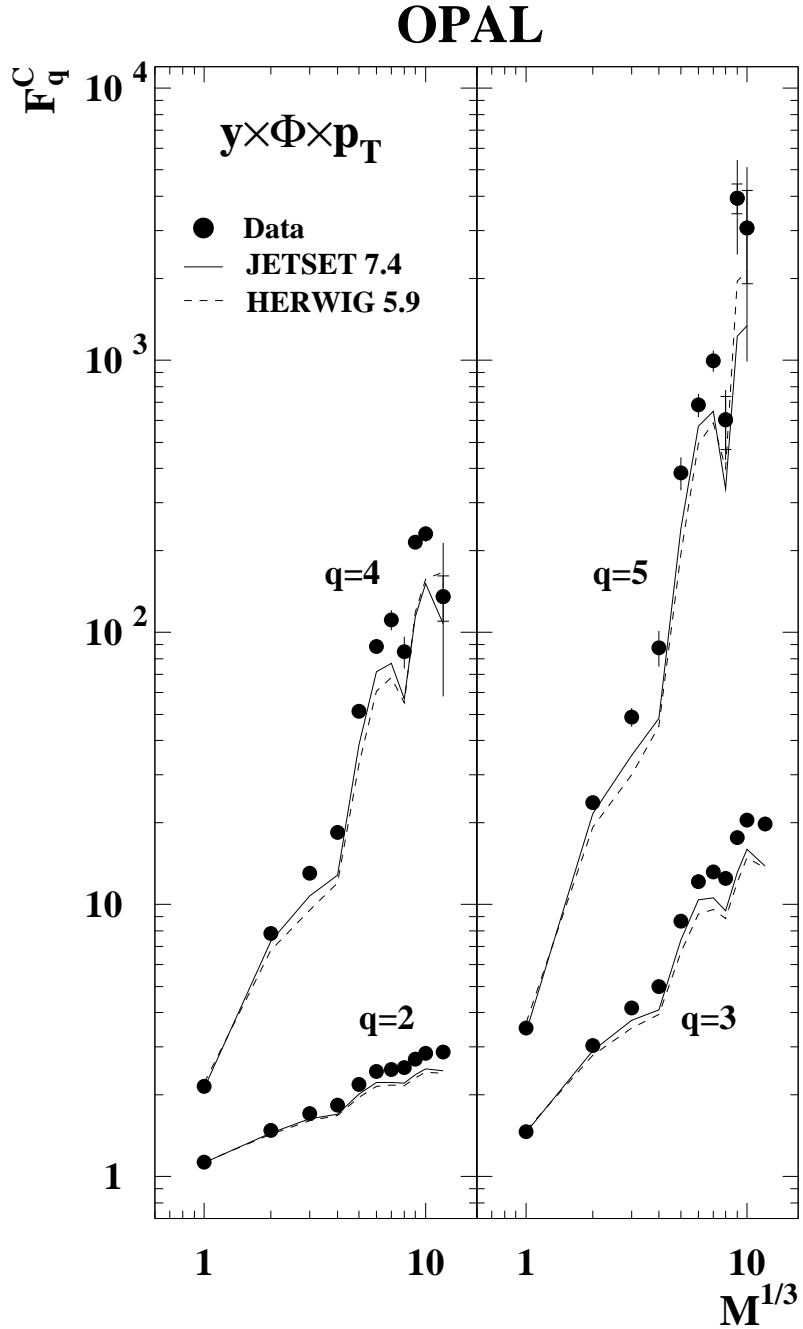


Figure 4: Factorial moments of order $q = 2$ to 5 vs. $\sqrt[3]{M}$, where M is the number of bins of the three-dimensional rapidity, azimuthal angle, and transverse momentum phase space, in comparison with the predictions of two Monte Carlo models. The total error is shown along with the statistical error (inner error bars) for each point.

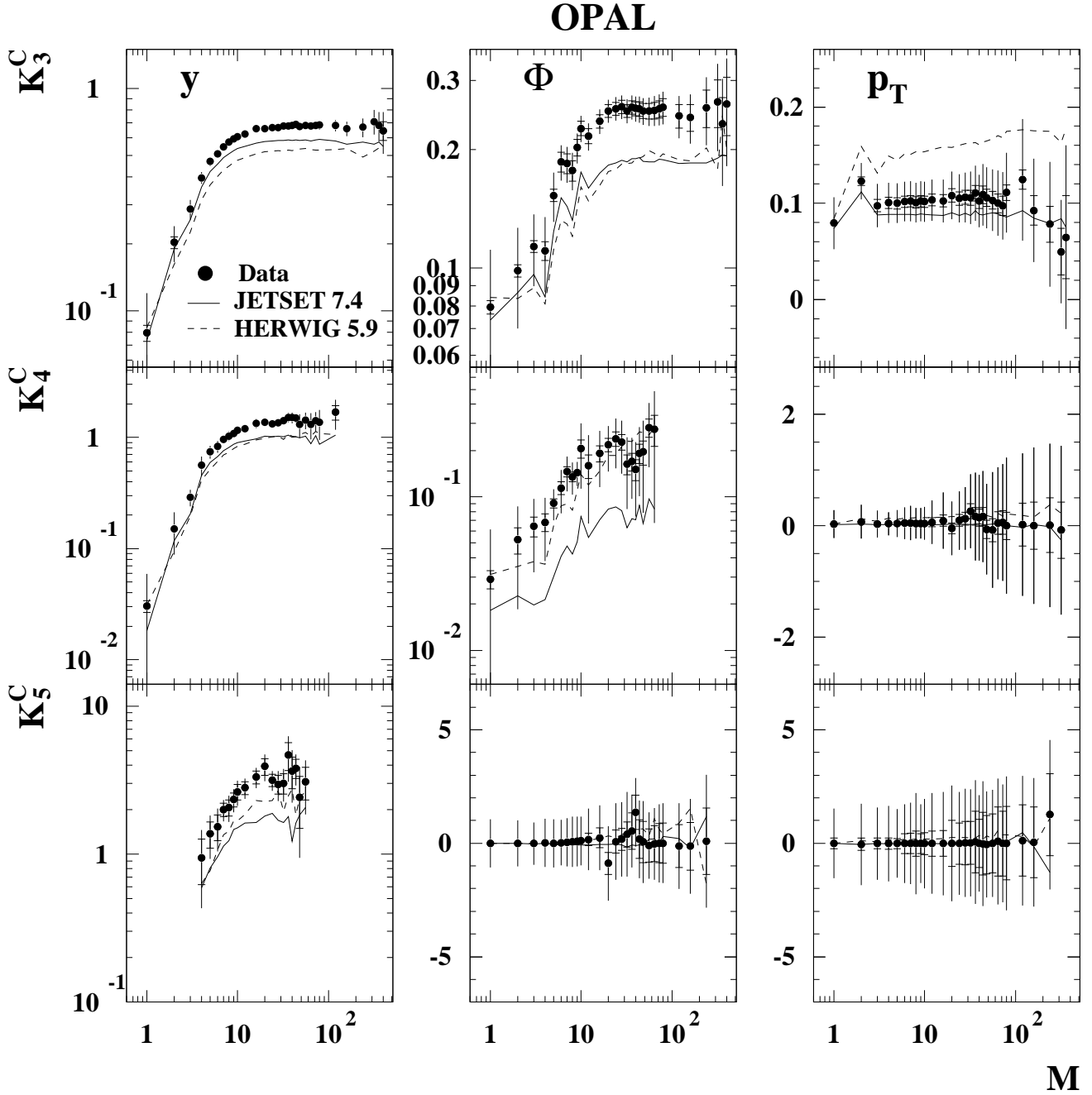


Figure 5: *Cumulants of order $q = 3$ to 5 vs. the number of bins M of the one-dimensional rapidity, azimuthal angle, and transverse momentum subspaces in comparison with the predictions of two Monte Carlo models. The total error is shown along with the statistical error (inner error bars) for each point.*

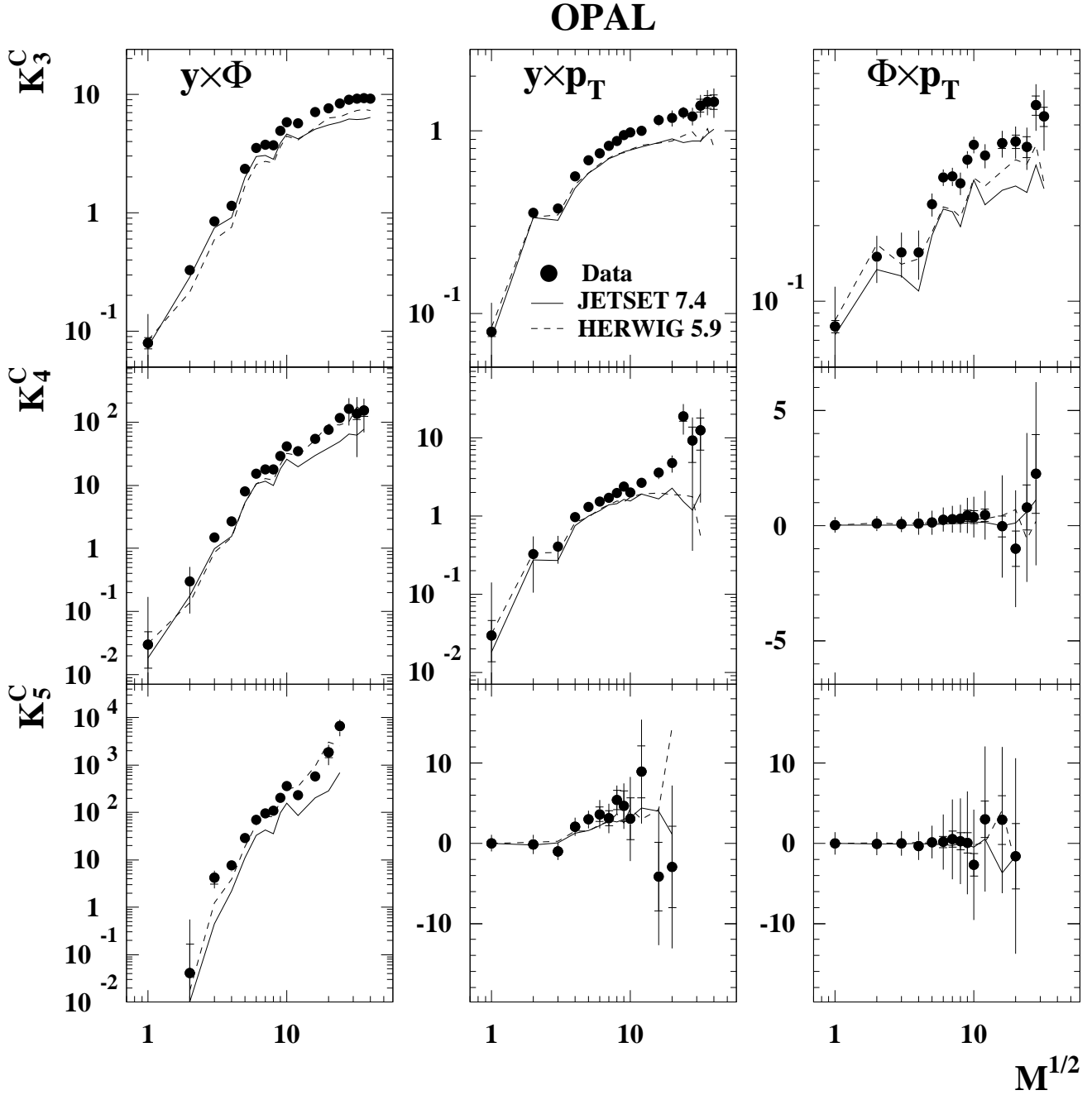


Figure 6: Cumulants of order $q = 3$ to 5 vs. \sqrt{M} , where M is the number of bins of the two-dimensional subspaces of rapidity, azimuthal angle, and transverse momentum combinations, in comparison with the predictions of two Monte Carlo models. The total error is shown along with the statistical error (inner error bars) for each point.

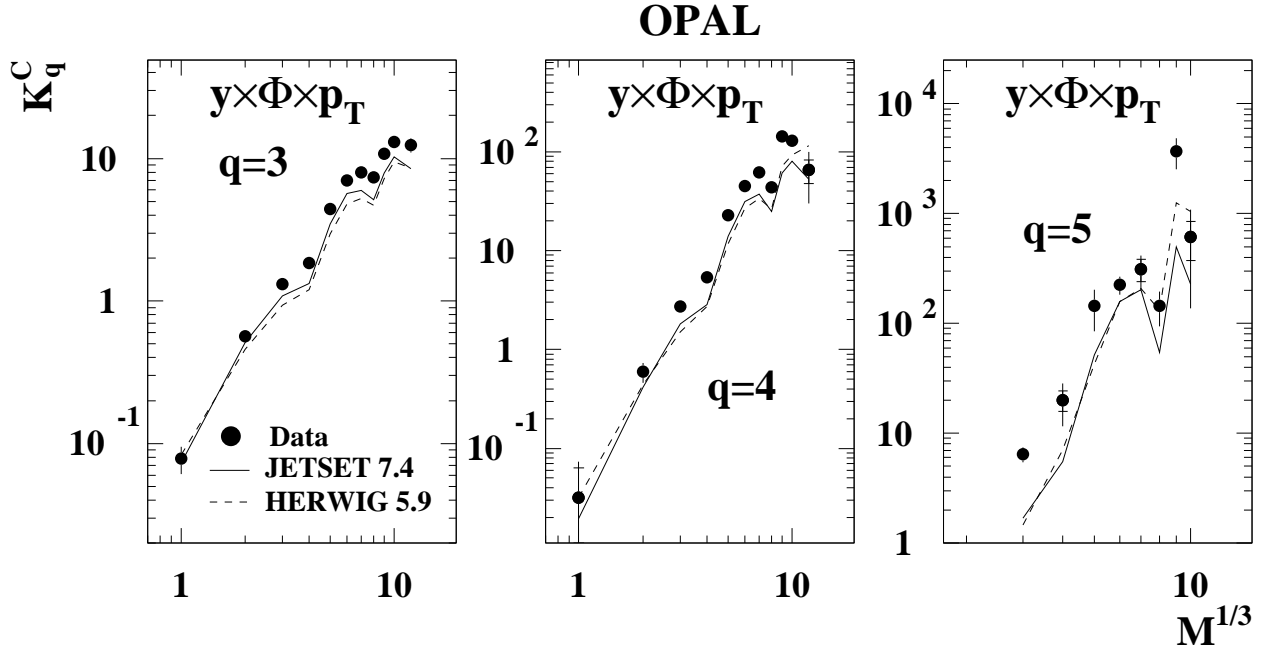


Figure 7: Cumulants of order $q = 3$ to 5 vs. $\sqrt[3]{M}$ where M is the number of bins of the three-dimensional rapidity, azimuthal angle, and transverse momentum phase space, in comparison with the predictions of two Monte Carlo models. The total error is shown along with the statistical error (inner error bars) for each point.

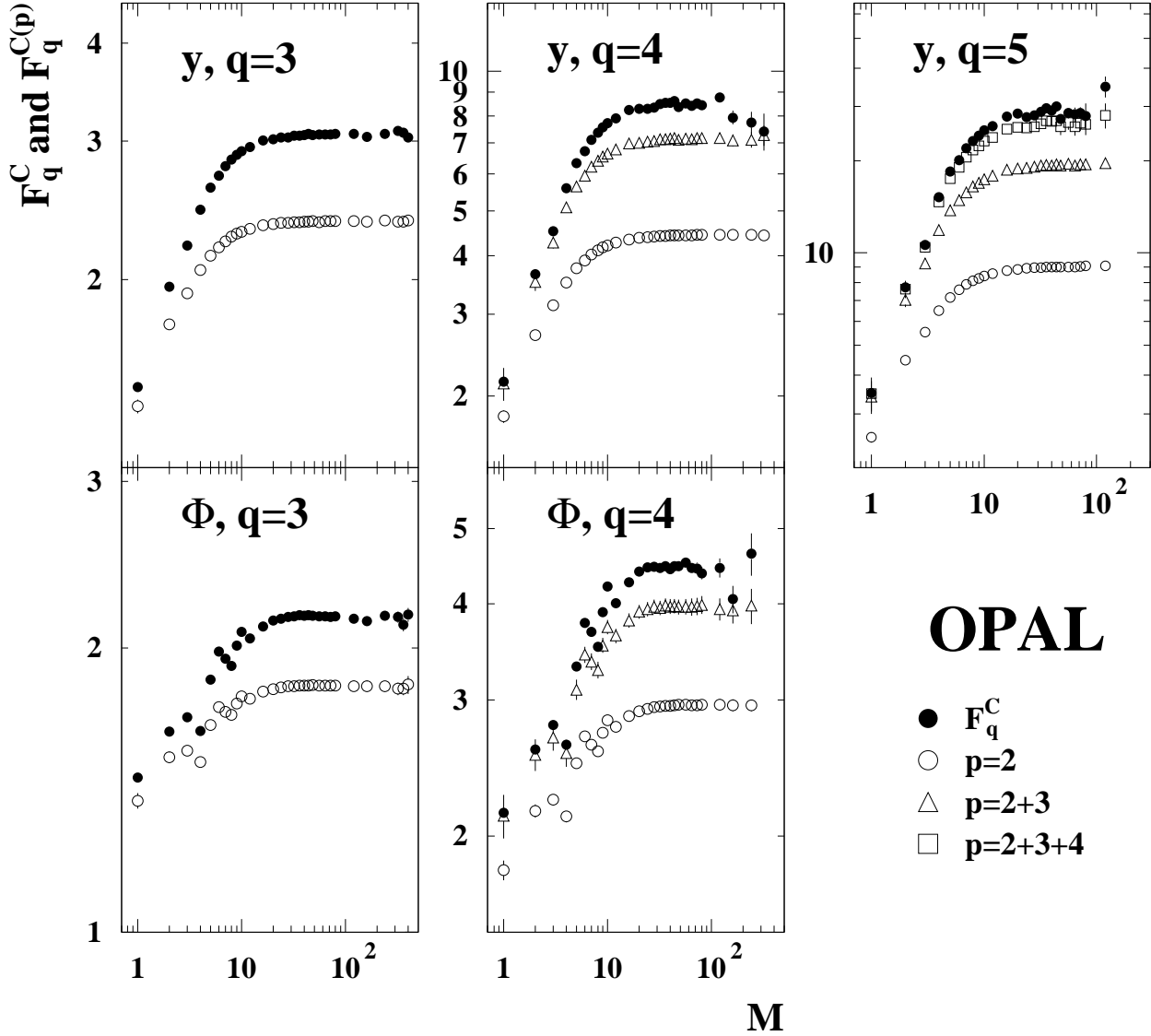


Figure 8: *Decomposition of the factorial moments F_q^C into multiparticle correlation contributions $F_q^{C(p)}$ in the one-dimensional rapidity and azimuthal angle subspaces. The error bars show the total uncertainties.*

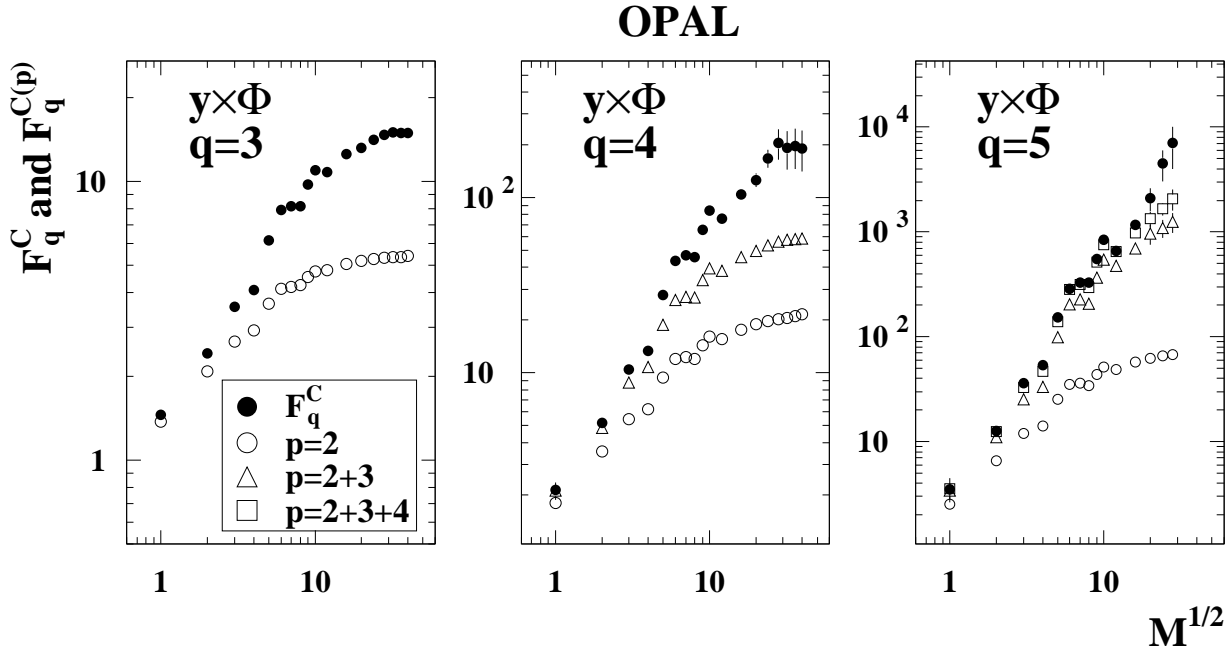


Figure 9: *Decomposition of the factorial moments F_q^C into multiparticle correlation contributions $F_q^{C(p)}$ in the two-dimensional subspace of rapidity and azimuthal angle. The error bars show the total uncertainties.*

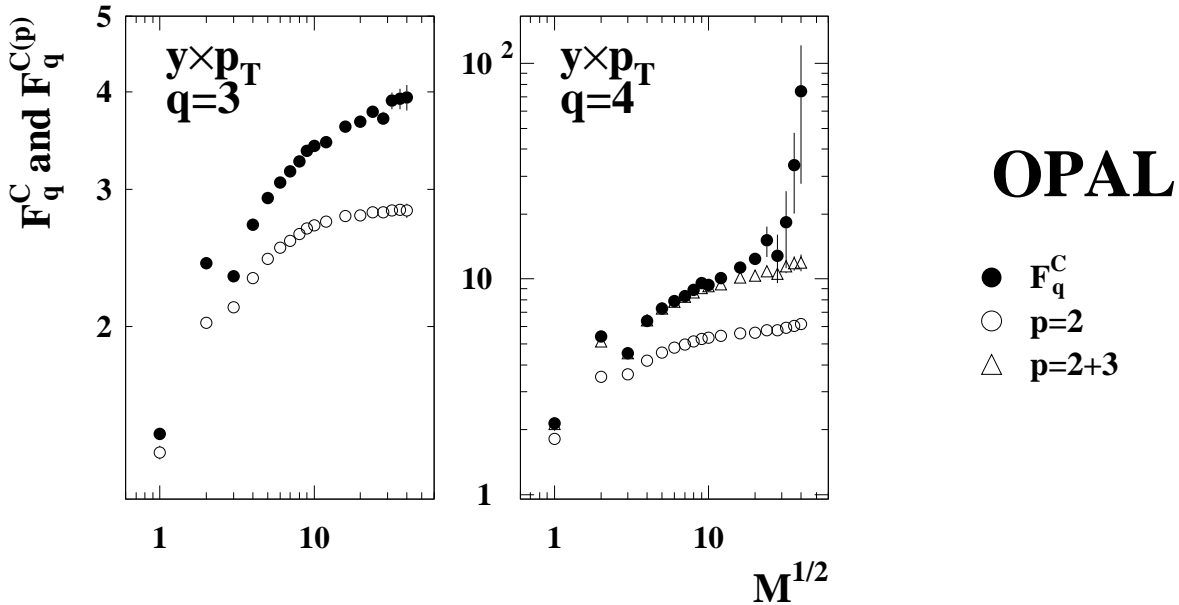


Figure 10: *Decomposition of the factorial moments F_q^C into multiparticle correlation contributions $F_q^{C(p)}$ in the two-dimensional subspace of rapidity and transverse momentum. The error bars show the total uncertainties.*

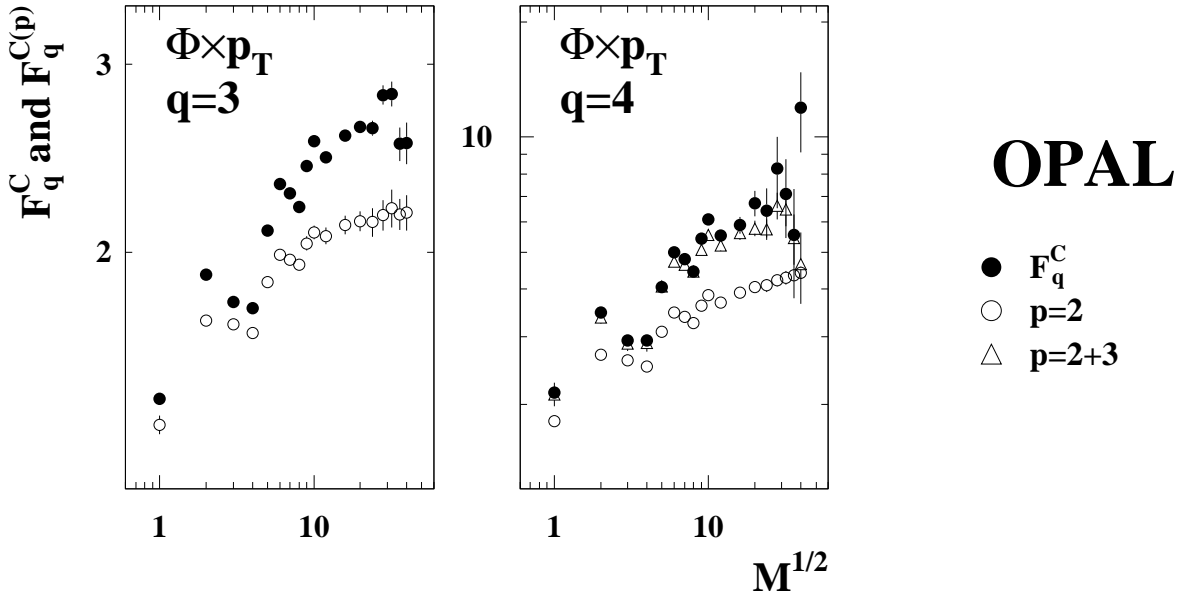


Figure 11: *Decomposition of the factorial moments F_q^C into multiparticle correlation contributions $F_q^{C(p)}$ in the two-dimensional subspace of azimuthal angle and transverse momentum. The error bars show the total uncertainties.*

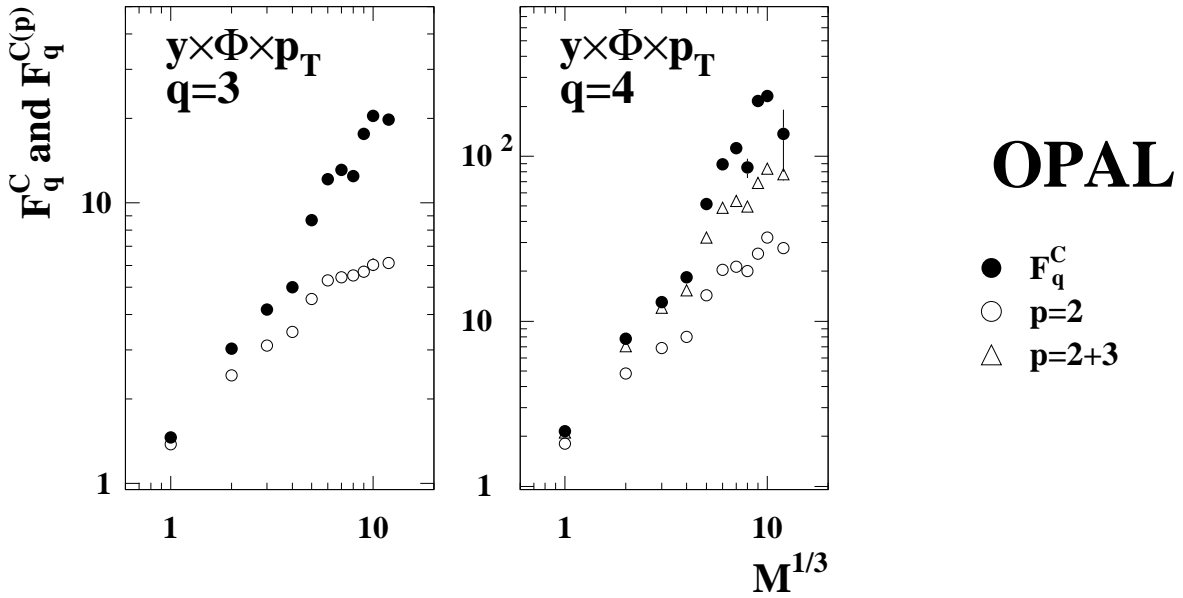


Figure 12: *Decomposition of the factorial moments F_q^C into multiparticle correlation contributions $F_q^{C(p)}$ in the three dimensions. The error bars show the total uncertainties.*